AIP Review of Scientific Instruments

Two dimensional triangulation of breakdown in a high voltage coaxial gap

S. W. Cordaro, S. C. Bott-Suzuki, L. S. Caballero Bendixsen, Levon Atoyan, Tom Byvank, William Potter, B. R. Kusse, and J. B. Greenly

Citation: Review of Scientific Instruments **86**, 073503 (2015); doi: 10.1063/1.4923459
View online: http://dx.doi.org/10.1063/1.4923459
View Table of Contents: http://scitation.aip.org/content/aip/journal/rsi/86/7?ver=pdfcov
Published by the AIP Publishing

REVIEW OF SCIENTIFIC INSTRUMENTS **86**, 073503 (2015)

Two dimensional triangulation of breakdown in a high voltage coaxial gap

S. W. Cordaro,[1,a)] S. C. Bott-Suzuki,[1] L. S. Caballero Bendixsen,[1] Levon Atoyan,[2] Tom Byvank,[2] William Potter,[2] B. R. Kusse,[2] and J. B. Greenly[2]
[1]*Center for Energy Research, University of California San Diego, San Diego, California 92093, USA*
[2]*Laboratory for Plasma Studies, Cornell University, Ithaca, New York 14853, USA*

(Received 16 April 2015; accepted 23 June 2015; published online 6 July 2015)

We describe a technique by which magnetic field probes are used to triangulate the exact position of breakdown in a high voltage coaxial vacuum gap. An array of three probes is placed near the plane of the gap with each probe at 90° intervals around the outer (anode) electrode. These probes measure the azimuthal component of the magnetic field and are all at the same radial distance from the cylindrical axis. Using the peak magnetic field values measured by each probe, the current carried by the breakdown channel, and Ampères law we can calculate the distance away from each probe that the breakdown occurred. These calculated distances are then used to draw three circles each centered at the centers of the corresponding magnetic probes. The common intersection of these three circles then gives the predicted azimuthal location of the center of the breakdown channel. Test results first gathered on the coaxial gap breakdown device (240 A, 25 kV, 150 ns) at the University of California San Diego and then on COBRA (1 MA, 1 MV, 100 ns) at Cornell University indicate that this technique is relatively accurate and scales between these two devices. © *2015 AIP Publishing LLC.* [http://dx.doi.org/10.1063/1.4923459]

I. INTRODUCTION

Vacuum gap breakdown mechanisms for many geometries, such as sphere-sphere, plane-plane, and point-plane, are well understood and documented.[1] To date, no detailed analysis of a coaxial geometry has been performed. This work is motivated by the need to better understand the mechanisms by which breakdown initiation occurs in a coaxial gap over a few nanoseconds to a few microseconds at tens of kV at gap sizes up to 1 mm, especially considering how common the use of a coaxial gap is in high voltage power lines of large pulsed power machines. Of specific interest is the location of breakdown about the azimuth, and the method by which this location can be determined. Any asymmetry in breakdown about the azimuth could be responsible for non-uniform distributions of voltage and current which could lead to early time scale instabilities of the load in question.

This work is relevant to larger pulsed power machines that presently make use of a μm high voltage coaxial vacuum gap in the power feed, such as the MagLIF[2] design on Sandia's Z-machine. On these larger machines, the cathode gap power feed cannot be observed and is often not directly monitored by diagnostic tools. Therefore, a comprehensive method to determine the location of breakdown by means other than axially aligned optical imaging would be beneficial.

II. EXPERIMENTAL DESIGN

An experimental system has been developed at the University of California San Diego to study the mechanisms and influences of coaxial geometry vacuum gaps. This table top experiment, the Coaxial Gap Breakdown (CGB) machine, consists of two aluminium electrodes; a hollow cylinder (R_{outer} = 6.09 mm-anode) with an inserted solid cylinder (R_{inner} = 5.19 mm-cathode) both of which are attached to 3-D translational mounts so as to ensure the electrodes are parallel to one another (Figure 1). Experiments were performed under vacuum (<10^5 Torr) and at room temperature. A high voltage pulse (25 kV, 150 ns) is delivered via charge circuit to the coaxial gap driving 240 A through the gap, with a few seconds between shots (limited by data collection speed). The vacuum gap was monitored by diagnostics including current measurement via Pearson coil (model 6585, 1.5 ns rise time), time integrated optical imaging, magnetic field measurements via B-dot probes, Mach-Zehnder interferometry via 532 nm, 0.4 ns pulse laser. In addition to the 900 μm gap used in this experiment, the CGB can accommodate any electrode geometry at gap sizes ranging from 25 μm to several millimeters. We also have the ability to heat the electrodes (up to 400 K), as well as rapid repetition rate (10–20 Hz) conditioning of electrodes.

Through experimentation on the CGB, a comprehensive method to determine the exact location of breakdown in a coaxial gap has been developed using an array of magnetic field (B-dot) probes. Magnetic field probes are made using semi-rigid coaxial cable (rg405/u). The cable is cut to the dimensions specified in Figure 2. The inner wire of the coaxial cable is wrapped in a kapton layer to ensure that each loop does not touch and prevent any breakdown between them. The area of each loop is made in the same fashion by wrapping the loops around an uncut semi-rigid coaxial cable of diameter 3.56 mm. The number of loops on each probe is determined by the operating conditions of the experiment. In this case, it was determined that for the CGB (220 A, 25 kv, 100 ns) a three loop probe 2-4 mm away was the optimal

[a)]scordaro@ucsd.edu. URL: http://www.P3ucsd.com.

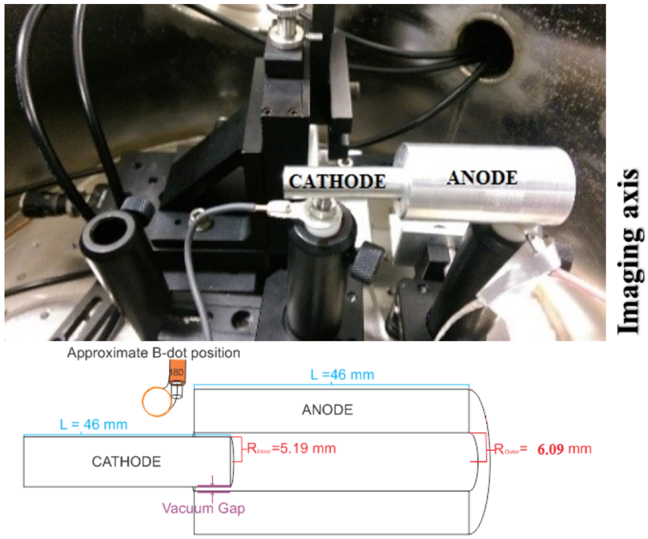

FIG. 1. CGB electrode orientation.

setup. Furthermore, it is very important that the connection of the loop to the outer shielding of the coaxial cable is sound as this reduces noise of the measured magnetic field signal.

Probes are calibrated through direct area measurement of the coils on each probe, with final sensitivity of each probe determined by a short circuit on the CGB machine. Starting with a known short circuit current pulse and known location of the center of B-dot probes with respect to the center of the electrode setup before the shot, we can calculate the expected magnetic field signals for each probe (Figure 3). Comparing the expected signals to those of the measured signals (Figure 4) we find that generally the measured signals match closely with both the current trace and the expected signals. Upon closer inspection we find that the percent difference away from expected values of each probe is less than five percent, these percent difference values are then added to the calculated calibration factor of each probe to ensure a complete and

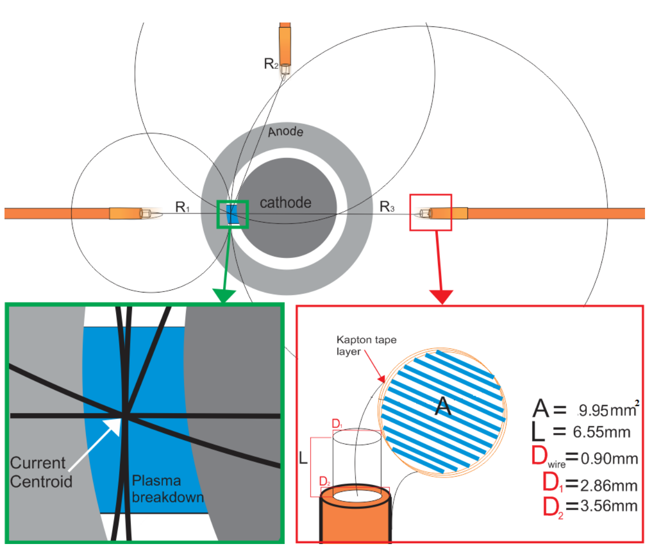

FIG. 2. Experimental setup diagram.

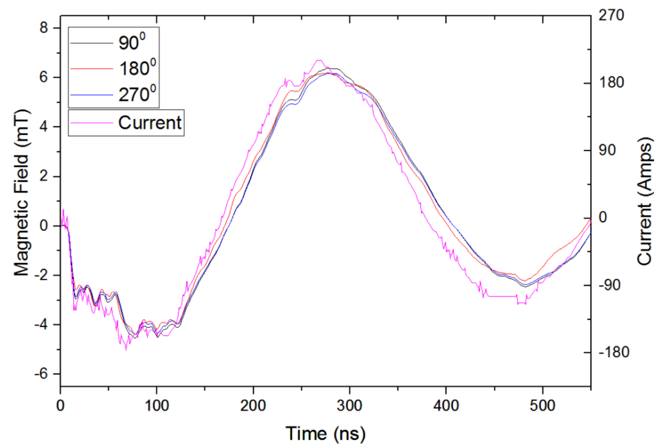

FIG. 3. CGB typical measured short circuit current and magnetic field calibration signals.

accurate calibration. This small percent difference indicates that the direct area measurement is rough yet sufficient alone to calibrate accurate B-dot probes.

In order to triangulate the location of breakdown we first calculate the magnetic field at peak current, by use of Equation (1), where V is the measured voltage generated by the magnetic field flux through a loop of area A, and N is the number of loops. Then, we take the calculated magnetic field for each B-dot probe, and use it to calculate the distance away (R) the breakdown occurred from the probe by use of Equation (2) at peak current (I),

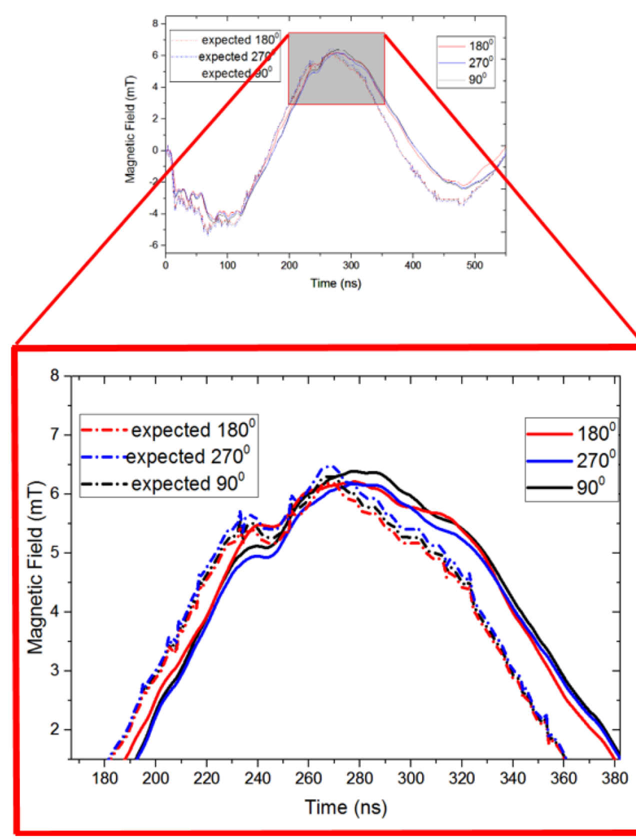

FIG. 4. CGB measured vs. analytical magnetic field calibration signals.

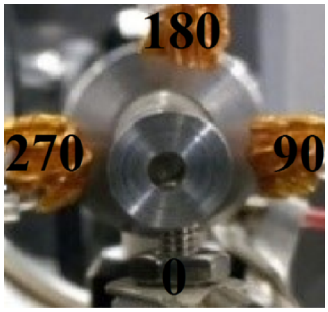

FIG. 5. Standard B-dot placement on the CGB.

$$V_{gen} = -N\frac{\mathrm{d}\Phi}{\mathrm{d}t} \rightarrow B = \frac{1}{AN}\int V dt, \quad (1)$$

$$\oint B \cdot dL = I_{enc} \rightarrow R = \frac{\mu I}{2\pi B}. \quad (2)$$

By generating three circles with origins located in the center of the corresponding B-dot loop of each probe, and radii corresponding to the different distance away from breakdown (R) for each probe, the intersection of these three circles can be observed and thus triangulate the absolute position at which the breakdown has occurred. When the triangulation data are overlaid on corresponding time integrated optical images, it is observed that the triangulation method determines the exact position that the breakdown has occurred. The accuracy of the 3 probe triangulation method means that the technique can be used to determine the exact position of a single breakdown in a coaxial gap even when time integrated axial optical emission imaging is not possible.

In order to maximize the effective mapping area of a coaxial gap, a minimum of three B-dot probes placed at 90° intervals around the circumference of the anode (Figure 5) is needed. The distance away from the anode each probe is placed is determined by the experiment and the sensitivity of the probes. Due to the location of the B-dot probes with respect to the vacuum gap, the probes do not read magnetic field signals generated by the radial current vectors of the breakdown.

To illustrate this technique, we have performed an analytical calculation of the triangulation method on a single breakdown occurring at the 90° probe side. We assume that each of the three probes is set with the same R value away from the center of the CGB, and that all of the current is distributed through the single breakdown point only. In order to accurately simulate a current pulse from the CGB, an approximation fit was performed on a typical operating current trace. With this approximated current signal, the peak magnetic field was then calculated using the peak current value and distances the

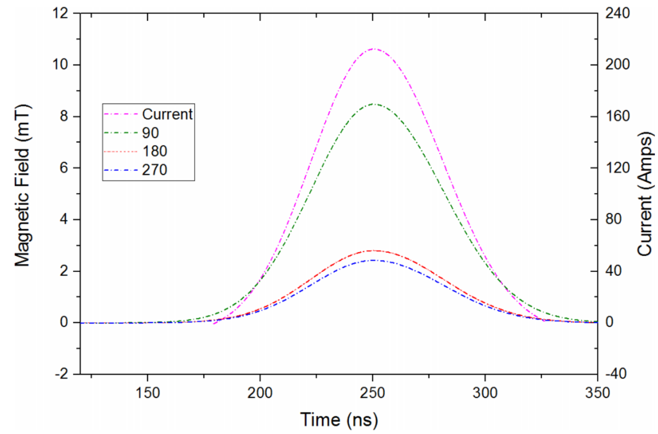

FIG. 6. Analytical curves for a breakdown at the 90° position.

probe center was located from the middle of the breakdown (Table I). These calculated magnetic field values were then used to simulate what the magnetic field trace would look like for each probe (Figure 6).

From Figure 6, it can be seen that the 90° probe reads the largest magnetic field, followed then by the 180° probe and the 270° probe. The analytical probe readings were then overlaid atop experimental probe readings from a shot in which breakdown only occurred at the 90° probe side (Figure 7). The resultant figure shows in general that all three probes have the same form and magnitude as analytical calculations, with a maximum error of 13%.

The triangulation technique was then performed on the measured magnetic field signals corresponding to shot no. 34, with the calculated distance away from breakdown values in Table I. The corresponding positioning circles were then overlaid atop time resolved optical imaging for the shot (Figure 8) accurately lining up with the exact position at which the breakdown occurred. The differences in distances and peak magnetic field in Table I are not an issue if the probe placement away from the experiment is known from either careful placement or optical imaging before the shot. Furthermore, because these distances are a known quantity the probe placement about the azimuth is irrelevant as it does not affect the triangulation technique. Though, it should be noted that placing probes closer than 30° from one another makes the resultant images more difficult to interpret.

We then apply the technique to the signals shown in Figure 9, where the 90° probe and 180° probe are greater than that of the 270° probe. Applying now the triangulation technique to the measured peak magnetic field values, we can find the corresponding distances away from breakdown

TABLE I. Analytical and measured values of shot no. 34.

Probe	Analytical magnetic field (mT) peak (250 ns)	Measured magnetic field (mT) peak (250 ns)	Calculated distance away (R) (mm)	Analytical distance away (R) (mm)
180	2.80	2.71	16.2	15.13
90	8.48	7.12	6.17	5.0
270	2.42	1.83	24.02	17.52

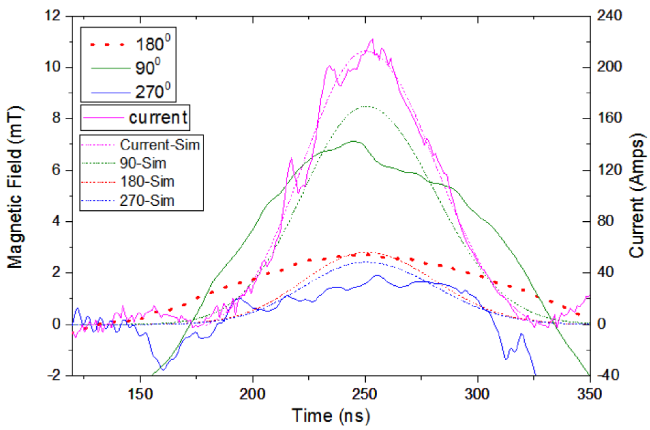

FIG. 7. Experimental vs. analytical magnetic field and current, shot no. 34.

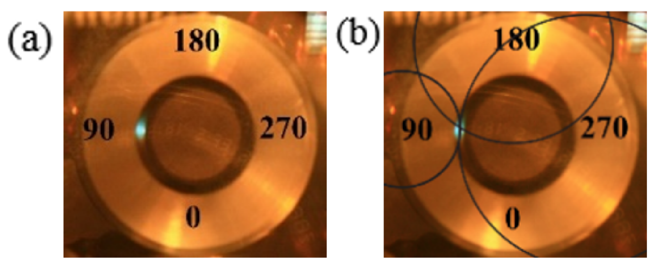

FIG. 8. Visualization of breakdown triangulation shot no. 34.

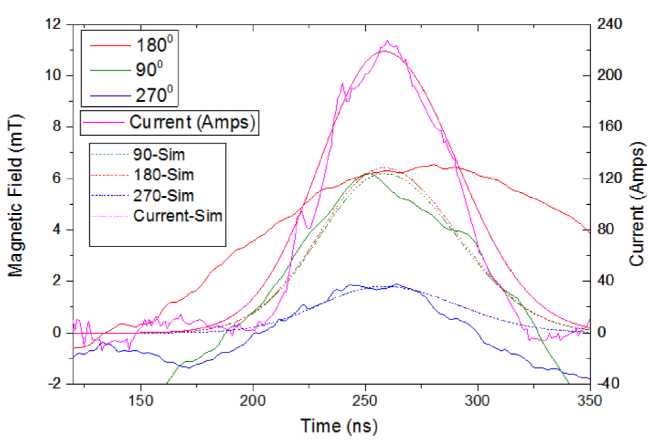

FIG. 9. Experimental vs. analytical shot magnetic field and current, shot no. 45.

that each probe is located (Table II). With these calculated values we can now generate our three circles and overlay them atop their corresponding probe centers in the shot specific time integrated optical image (Figure 10(b)). As seen from

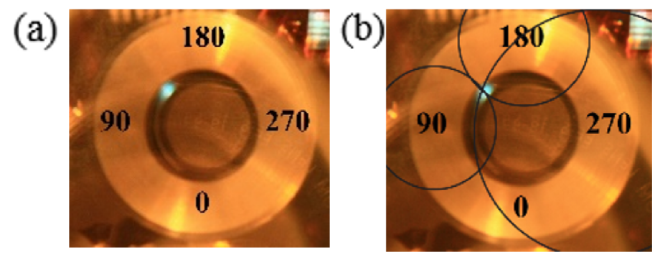

FIG. 10. Visualization of breakdown triangulation shot no. 45.

the triangulation cartoon, the centroid of the breakdown was accurately determined by the technique.

III. IMPLEMENTATION ON MEGA-AMPERE MACHINE

A second series of experiments was carried out on COBRA[3] (1.1 MA, 100 ns rise time) at Cornell University, the first such attempt to determine how well the B-dot triangulation technique scales to much larger devices. The technique was tested using the same probes used on the CGB but only a single loop. The entire loop of the probe was wrapped in kapton tape and coated in epoxy to ensure survival in such a harsh environment, similar to the probes[4] made at Cornell University. Analogous to the experiment on the CGB, probes are placed at 90° intervals around the AK gap of the COBRA machine, with each probe position away from the center of the experiment determined by pre-shot optical imaging (Figure 12). Due to the large amount of debris, the probes were replaced with identically calibrated probes after each shot. The single loop probes were calibrated using the Cornell B-dot calibration pulser (3 kA, 100 ns) prior to each shot. The experiment was monitored by axial gated imaging with a 12-frame high speed camera (10 ns exposure, Invisible Vision- Ultra UHSI 12/24) in order to monitor the gap for the duration of the current rise to peak (110 ns). An initial test of the triangulation technique was performed using a 250 μm aluminium wire offset towards the 90° probe (Figure 12(a)-left side) in order to ensure the centroid of the current is in a known location to test the calibration of the probes. The first plot in Figure 11 shows the corresponding magnetic field signals for the wire shot, the largest magnetic field occurs at the 90° probe indicating that the centroid of the current was offset towards that probe. This is confirmed when the triangulation technique is overlaid atop preshot optical imaging and compared to axially aligned 12 frame optical imaging (Figure 12(a)-right side). Subsequent experiments were performed on liners with gap sizes analogous to those used on the CGB experiment. A shot of particular

TABLE II. Analytical and measured values of shot no. 45.

Probe	Analytical magnetic field (mT) peak (250 ns)	Measured magnetic field (mT) peak (250 ns)	Calculated distance away (R) (mm)	Analytical distance away (R) (mm)
180	6.40	6.41	6.86	7.04
90	6.19	6.21	7.11	7.08
270	1.81	1.81	24.3	24.3

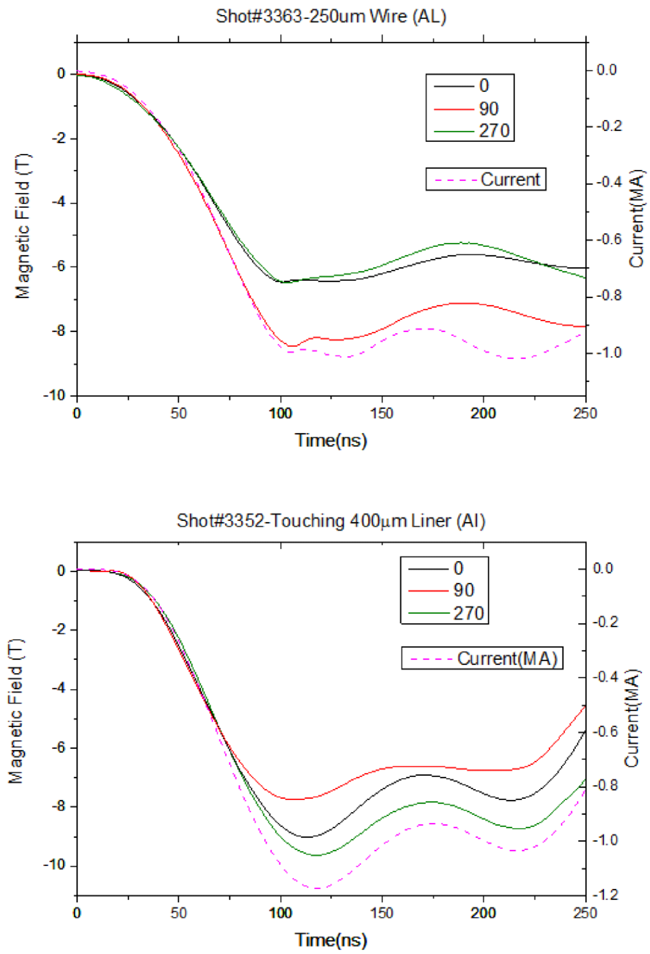

FIG. 11. COBRA magnetic field and current signals.

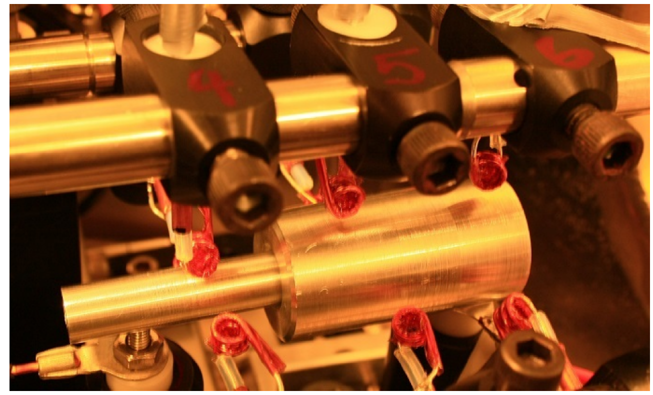

FIG. 13. Nine probe B-dot array.

interest was done with an aluminium liner (400 μm gap) offset to touch the edge nearest the 180° probe side. The second plot in Figure 11 shows the corresponding magnetic field signals of the touching liner shot. The triangulation technique was then applied and overlaid atop preshot optical imaging and compared to axially aligned 12 frame optical imaging (Figure 12(b)). It can be seen that the centroid of the current was indeed located at the contact point of the liner at the 180° probe side. The red circle (Figure 12(b)-left side) in the triangulation shot represents the actual position of the liner when the imaging angle is corrected.

IV. DISCUSSION

We have shown that with the use of a minimum of three B-dot probes one can determine the exact location at which a breakdown has occurred within a coaxial gap by taking the magnetic field values at peak drive current, with a calculated error of up to 13%, to determine the distance away each probe is from the breakdown, and that the technique scales well to larger devices.

It is important to note, however, that the three probe triangulation accuracy diminishes under certain conditions, changing from an exact location to an effective area at which breakdown occurs. For instance, when the depth into the plane (Figure 8 or 10) of the gap is sufficiently long ($L \gg 5$ mm) the two-dimensional triangulation technique cannot accurately

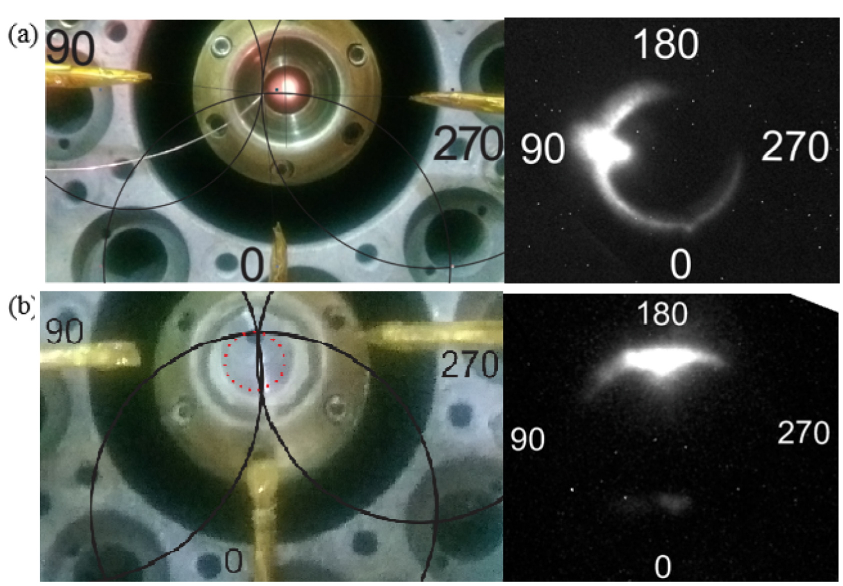

FIG. 12. Triangulation visualization Cornell experiment.

detect the variations of magnetic field corresponding to breakdowns occurring along the length of the electrode. Furthermore, when multiple breakdowns occur about the azimuth of the coaxial gap the variations of the magnetic field become less dramatic, resulting in multiple intersection points that represent an area at which breakdown has occurred. Improvements to the coaxial experiment are currently underway to understand and resolve the effects of multiple breakdowns on the evolution and distribution of magnetic field strength through the use of a nine B-dot probe array placed along the length of the coaxial gap (Figure 13) to determine the triangulation of breakdowns along the length of the electrodes through a 3D mapping of the magnetic field. This B-dot probe array will allow for a better understanding of the evolution and dynamics of the breakdown in the coaxial geometry. Furthermore, the technique will be applied to magnetic field values along the rising edge of the current profile so as to study change in position of the breakdown as a function of time.

ACKNOWLEDGMENTS

Work was supported under the NNSA SSAA program through DOE Cooperative Agreement No. DE-FC03-02NA00057.

[1]M. Okawa, T. Shioiri, H. Okubo, and S. Yanabu, IEEE Trans. Electr. Insul. **23**(1), 77 (1988).
[2]S. A. Slutz, M. C. Herrmann, R. A. Vesey, A. B. Sefkow, D. B. Sinars, D. C. Rovang, K. J. Peterson, and M. E. Cuneo, Phys. Plasmas **17**, 056303 (2010).
[3]J. B. Greenly, J. D. Douglass, D. A. Hammer, B. R. Kusse, S. C. Glidden, and H. D. Sanders, Rev. Sci. Instrum. **79**, 073501 (2008).
[4]J. Greenly, M. Martin, I. Blesener, D. Chalenski, P. Knapp, and R. Mcbride, AIP Conf. Proc. **1088**, 53 (2009).